RSC Advances

ROYAL SOCIETY OF CHEMISTRY

www.rsc.org/advances

Self-folding of Polymer Sheets Using Microwaves and Graphene Ink

Duncan Davis[1], Russell Mailen[2], Jan Genzer*[1], Michael D. Dickey,*[1]

[1] Department of Chemical and Biomolecular Engineering, NC State University
[2] Department of Mechanical and Aerospace Engineering, NC State University

Abstract

Self-folding represents an attractive way to convert two-dimensional (2D) material sheets into three-dimensional (3D) objects in a hands-free manner. This paper demonstrates a simple approach to self-fold thin pre-strained polystyrene (PS) sheets using microwaves. While the PS sheets are transparent to microwaves, patterns of screen-printed ink containing graphene absorb microwaves and cause the underlying printed sections of the sheet to warm up. When the local temperature in the inked region exceeds the glass transition temperature of PS (~103°C), the strain in the inked regions of the film relaxes gradually across the sheet thickness, which causes the PS sheet to fold. The resulting dihedral angle is proportional to the width of the hinge printed by graphene ink. The geometry and azimuthal orientation of the sample inside the microwave reactor affect the quality of the folding due to the non-uniformity of the microwave energy inside the reactor. While self-folding has previously utilized heat, light, photo-chemistry, and solvent swelling, this paper reports the use of microwaves, which can deliver large amounts of energy remotely.

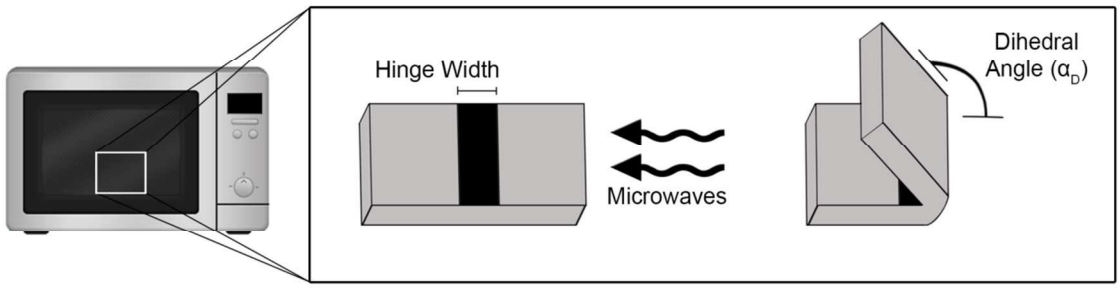

*Corresponding authors: jan_genzer@ncsu.edu, mddickey@ncsu.edu

Introduction

This paper describes the self-folding of polymer sheets using microwaves (frequency~2.45 GHz) as a heating source to achieve a wide range of dihedral angles that fold within seconds. Self-folding strategies convert planar surfaces into three-dimensional (3D) objects in a hands-free manner. Self-folding is attractive for a number of applications, including remote deployment of compact structures(1–3), assembly(4), packaging(5), robotics(6,7), mechanical metamaterials(8), and mechanical actuation(9). In general, sheets that self-fold have two common features: (1) a 'hinged' region that differs chemically, physically, or mechanically from the rest of the sheet, and (2) a force that arises in response to an external stimulus and causes the hinged region to fold. Previously, researchers induced self-folding using light(10–29), heat(9,28,30–37), lasers(38–43), pH(44), swelling(45–50), electricity(4,51–57), magnets(58–61), and pneumatics(62–64). This work demonstrates it is also possible to use microwaves to induce self-folding. Although there are a number of approaches to self-folding(65), the method described here is most closely related to those that utilize localized heating of shrink films (i.e., shape memory polymers) to induce folding (see reference 24 and those therein). In this context, microwaves are appealing because they can be generated easily to deliver large amounts of energy from large distances. Microwave ovens are also common household items and, in principle, could be utilized to convert flat objects shipped to the home into 3D objects.

Microwaves are electromagnetic waves with a frequency between 300 MHz and 300 GHz. Most commercial microwave ovens use a frequency of 2.45 GHz, including the one utilized in our studies. Microwaves deliver heat via dielectric heating (also known as electronic heating), which results from molecular dipoles in a material absorbing the microwaves and orienting themselves with or against the oscillating electric field(66–72). When the dipoles cannot re-orient as fast as the frequency of the electric field, they remain out of phase with the electric field created from the microwave(66–72). This lag (i.e., dielectric loss) causes energy to be dissipated in the form of heat. Thus, the dielectric loss of a material determines how much microwave energy a given material can absorb. While polymers generally do not absorb microwaves effectively, a number of materials absorb microwaves in a large extent, including graphene and graphite(68,71).

In this work, we utilize Vor-ink^{tm} as a microwave absorbing ink. This ink comprises a heterogeneous mixture that includes graphene, iron oxide, solvent, and polymer stabilizers. We chose this ink because it absorbs microwaves effectively, it is easy to pattern, and it is commercially available. We screen printed the ink on the surface of sheets of prestrained

polystyrene (PS) to create 'hinges' with well-defined geometry (i.e., size and position). Whereas many self-folding approaches utilize multi-step fabrication strategies to define hinges, the simple screen printing approach utilized here creates hinges in a single step on a commercially available, homogeneous plastic sheet. Previously, patterns of ink have been utilized to locally heat the underlying polymer by light absorption(24) and Joule heating(57). Here, the absorbance of microwaves by the ink causes the polymer underneath the ink to heat. When the local temperature in the sheet exceeds the glass transition temperature of PS (~103°C)(24), the strain in that region of the film relaxes in a gradual fashion across the sheet thickness, causing the PS sheet to fold in the direction towards the inked side of the sheet. Thus, the ink defines a hinge in the sheet and for the microwave power utilized here, the polymer folds over the course of 1-3 seconds starting from room temperature. This paper demonstrates self-folding of polymer sheets using microwaves and shows that the hinge geometry, the sample orientation in the microwave reactor, and the power of the microwave control the angle, times scales, and quality of the self-folding.

Results and Discussion

We first sought to demonstrate that it is possible to use microwaves to induce self-folding of polymer sheets. **Figure 1** shows schematically the process of creating and folding the samples. The substrates consist of prestrained polystyrene films (Shrinky Dink^{TM}, 300 μm thick) screen-printed with lines of graphene ink that also contains ~10 wt% iron oxide. A micrograph of a screen printed line is shown in **Figure S1** in the Supplementary Information. **Figure S2** in the Supplementary Information section depicts a typical height profile (~50 - 100 μm thick) of the ink that defines the hinge. Graphene and iron oxide both absorb microwaves strongly(68,71).

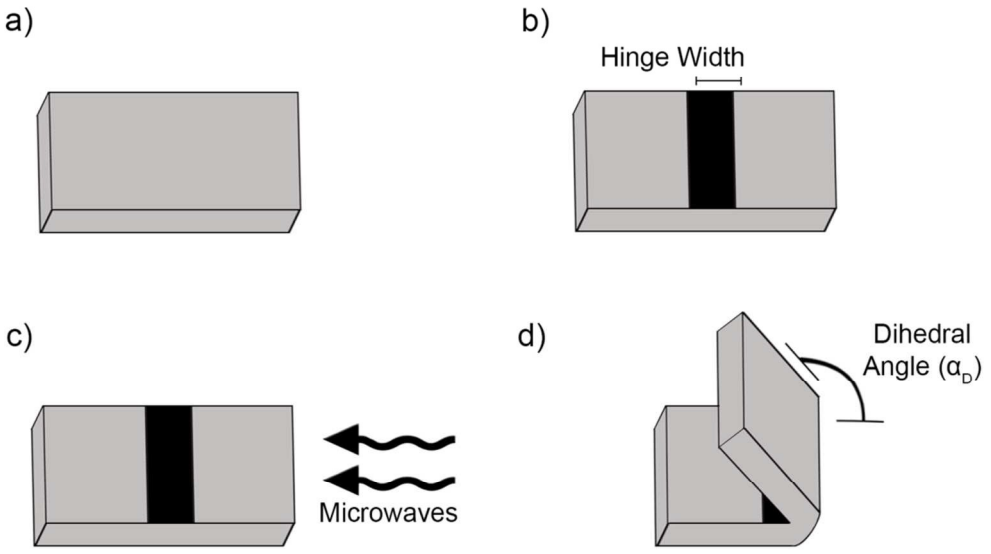

Figure 1. Folding process induced by microwaves (not to scale). A pre-strained polystyrene sheet (a) is screen-printed with graphene ink on the surface of the sheet (b); the printed regions define a 'hinge'. Microwaves heat the ink (c); the microwave source is physically positioned on the right side of the sample, but is designed to create a standing wave inside the vessel of the microwave reactor. The sample folds to a dihedral angle α_D due to the localized heating of the inked region in the sample via absorption of microwaves (d).

A microwave reactor heats the samples, which rest against the bottom of a cylindrical glass chamber inside the reactor (85 mm deep and 20 mm diameter). Microwave ovens designed for food operate at a power of 900 W, but the reactor here was operated at 250 W. We expose the samples to 250 W of power for up to 3 s, resulting in dihedral angles (α_D) ranging from 0° to 180° by varying only the hinge width, as shown in **Figure 2**. Shorter exposure times result in less folding. Times longer than 3 s often result in distorted samples and in some cases, ignition, which shows how effectively the ink absorbs the microwaves. The polymer portion of the sample is transparent to microwaves and consequently does not heat up. Supporting video S1 shows the folding of a polymer sheet in response to microwaves.

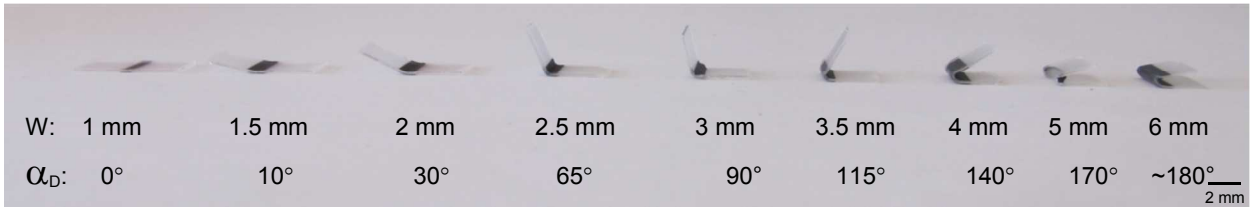

Figure 2. The maximum dihedral angle (α_D) increases with increasing hinge width (W). The samples are 6 mm wide in the dimension parallel to the hinge.

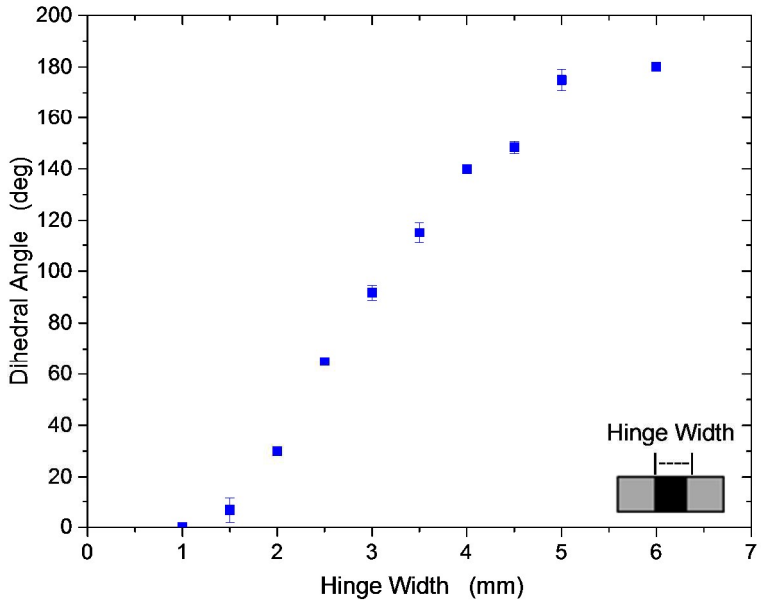

Figure 3. Dihedral angle (α_D) as a function of the hinge width (W). The error bars capture the first standard deviation with a minimum of 3 repetitions of each hinge width with all other variables held constant. These samples are all exposed to a microwave power of 250 W, an orientation of 90°, and a square-shaped hinge composed of graphene ink (see text).

Figure 3 depicts the near linear dependence of dihedral angle (α_D) on hinge width while keeping all other parameters constant. The error bars indicate the repeatability of the folding process. By varying only the hinge width, we can precisely control α_F to range from 0° to nearly 180°.

During these measurements, we observed that the folding behavior of the samples depends strongly on both the sample geometry and the in-plane (*i.e.*, azimuthal) orientation of the hinge inside the microwave reactor. Samples folded most reliably when oriented at 90°; i.e., with the long axis of the hinge aligned perpendicular to both the front panel of the instrument and therefore, perpendicular to the source of microwaves. **Figures 2** and **3** report the folding behavior of samples oriented azimuthally at 90°. We sought to understand why the other sample orientations folded poorly (azimuthal angle ~45°) or not at all (azimuthal angle ~0°) by varying systematically the orientation, geometry, and microwave power. We hypothesize that folding depends on sample orientation due to the non-uniformity of microwaves inside the reactor, which cause non-uniform heating of the hinge.

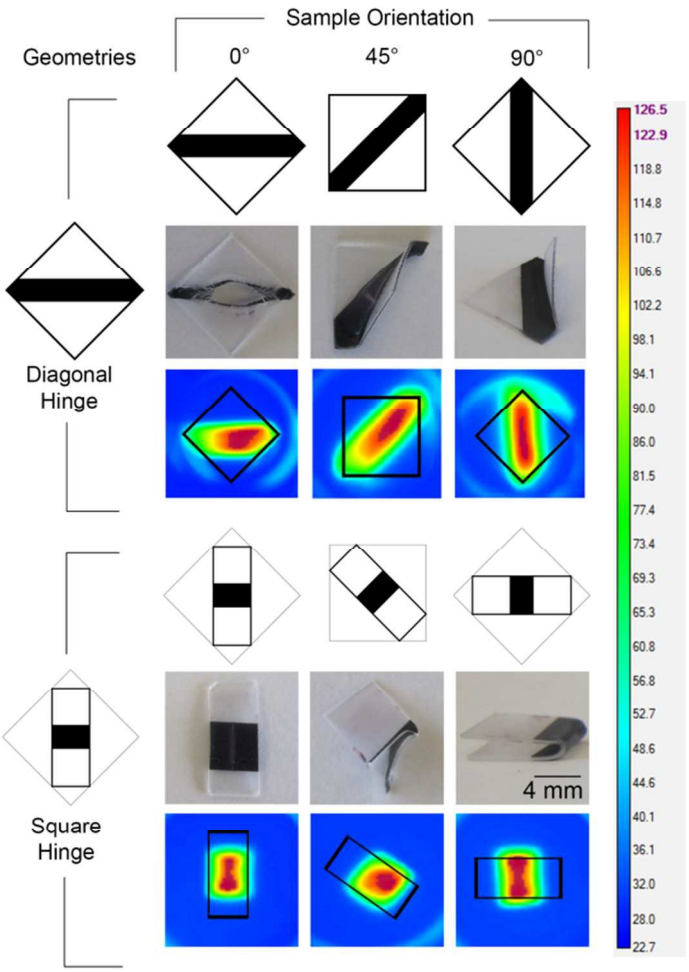

Figure 4. Two sample geometries ('diagonal hinge' and 'square hinge' groups) are depicted at 3 different sample orientations (columns) relative to the direction of the microwave source. The top row of each group is a cartoon of the sample, the middle row contains photographs of samples after exposure to 3 s of microwave, and the bottom row is an IR image of the sample slightly before it begins to move in response to microwaves (with the temperature scale on the right side).

We chose two different geometries in our study, as depicted in **Figure 4**. The diagonal hinge geometry spanned the diameter of the microwave vessel to explore the uniformity of the heating of the hinges. The diagonal hinge geometry consists of a 13 mm x 13 mm polystyrene square with a hinge spanning opposite corners. This sample had the maximum possible hinge length (17 mm) that can fit in the microwave without touching the vessel walls. The square hinge geometry consists of 13 mm x 6 mm PS rectangle with a centered, square-shaped hinge. The use of a square-shape minimizes the effect of orientation on the average temperature of the hinge but not its effect on folding.

The self-folding studied here is a thermally-driven process. To test if uneven heating causes variation in folding behavior with respect to sample orientation, we utilized an IR camera

to measure the surface temperature of the hinge during exposure to the microwaves. Changing the orientation of the samples changed the temperature profile of the hinge during the microwave heating. **Figure 5** plots the average temperature of the hottest region of the hinge versus time for each of the six possible combinations of sample geometry and orientation using samples with a 3 mm hinge width exposed to 250 W of microwave power. The 'square hinges' have temperature profiles that are nearly independent of orientation, whereas the profiles for 'diagonal hinges' vary with alignment. To quantify the heating rate of the surface, we fit the experimental data (cf. **Figure 5**) to a *tanh* function and define the maximum heating rate as a tangent at the inflection point of the *tanh* function (see **Figure S5** in Supporting Information). **Figure 6** plots the maximum heating rates for each sample configuration.

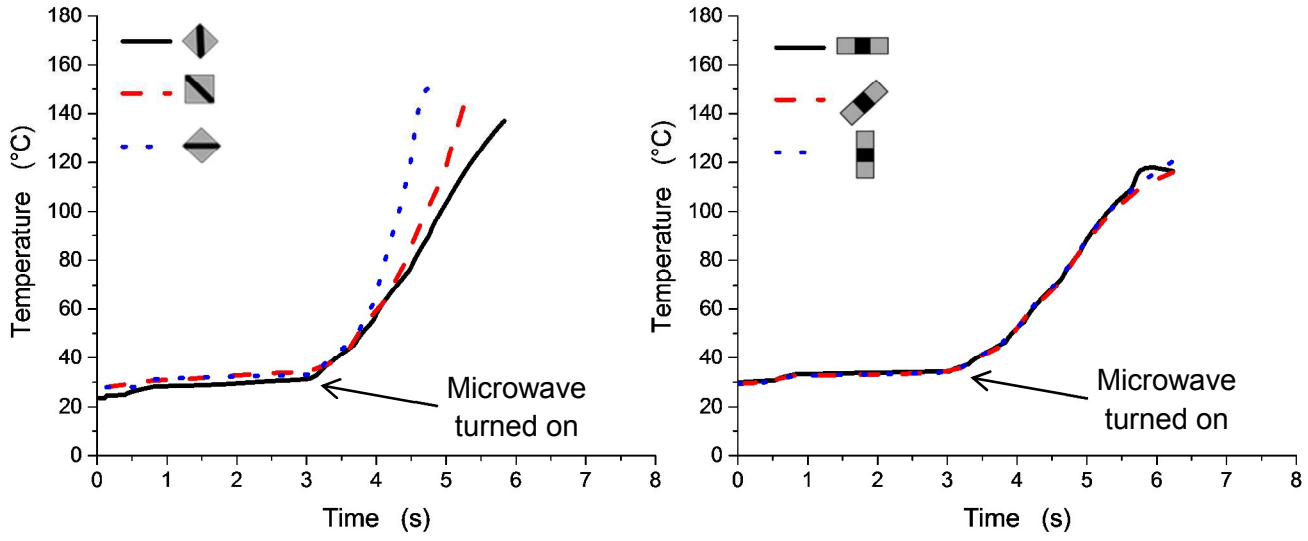

Figure 5. Time-dependence of temperature in a) 'diagonal hinge' samples with varying orientation and hinge width of 3 mm; b) 'square hinge' samples with hinge width of 3 mm. The microwave power is 250 W in both cases. The IR camera cannot measure accurately temperatures above 150°C and therefore the data truncates at that value.

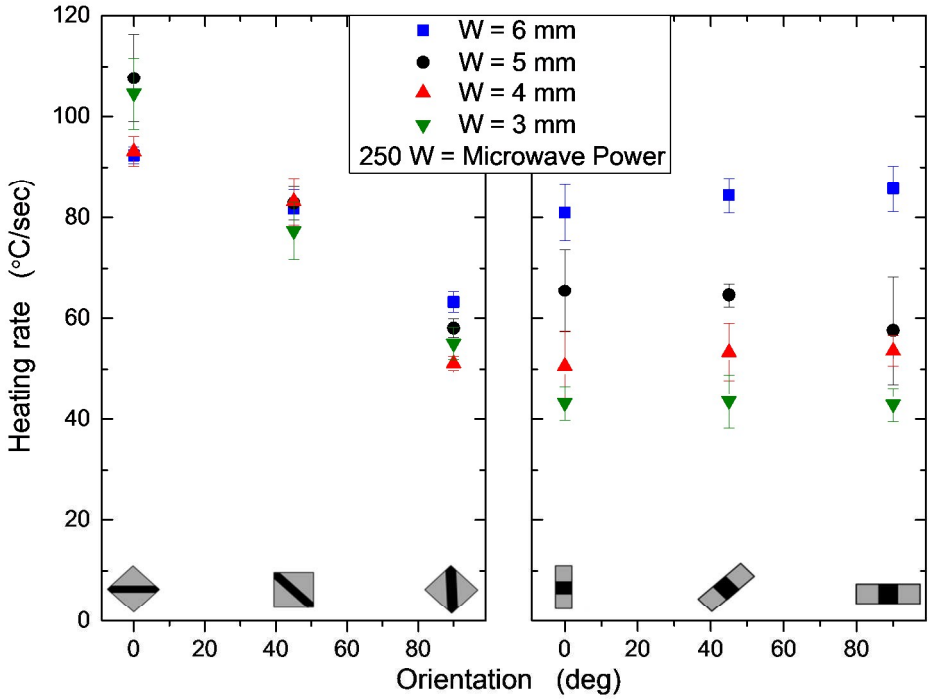

Figure 6. Heating rate of the samples at different orientation relative to the direction of the microwave radiation (azimuthal angle) and hinge widths (W) are shown.

The results in **Figure 6** confirm that the orientation affects the maximum heating rate of the samples with a 'diagonal hinge' more than the hinge width. Because the diagonal hinges span the walls of the reactor, this result suggests that there is a strong variation in microwave power around the perimeter of the reactor. Samples oriented at 0° and 45° did not heat uniformly along the long axis of the hinge (see **Figure S3** and **S4** in Supporting information and the images in **Figure 4**). This non-uniformity causes distortion (0° orientation) and off-center folding (45° orientation). We observed a few sparks during the folding of all three orientations but they were most pronounced during samples orientated at 0°. The sparks appear to partially ablate the ink for the 0° samples, but do not seem to affect the folding of 45° or 90° samples; eliminating sparks may be possible by optimizing the resistivity of the ink. In the square hinge samples, the orientation does not affect the maximum heating rate since the areal coverage of the graphene ink remains centered in the reactor regardless of orientation. For these samples, the hinge width affects the maximum heating rate much more than the sample orientation. The trends in the data shown in **Figure 6** also occur at 30 W microwave power (see Supporting Information).

The data in **Figure 6** motivated us to study the uniformity of the microwaves in the vessel. We mapped the heating profile inside the microwave using a paper (MWAC, Atlanta Chemical) that absorbs microwaves and changes color permanently due to thermal excursions above a temperature of 65°C. **Figure 7** shows pictures of the paper after exposure to different durations of microwave heating. The color 'front' propagates across the paper with time, illustrating the non-uniformity in the aerial microwave intensity.

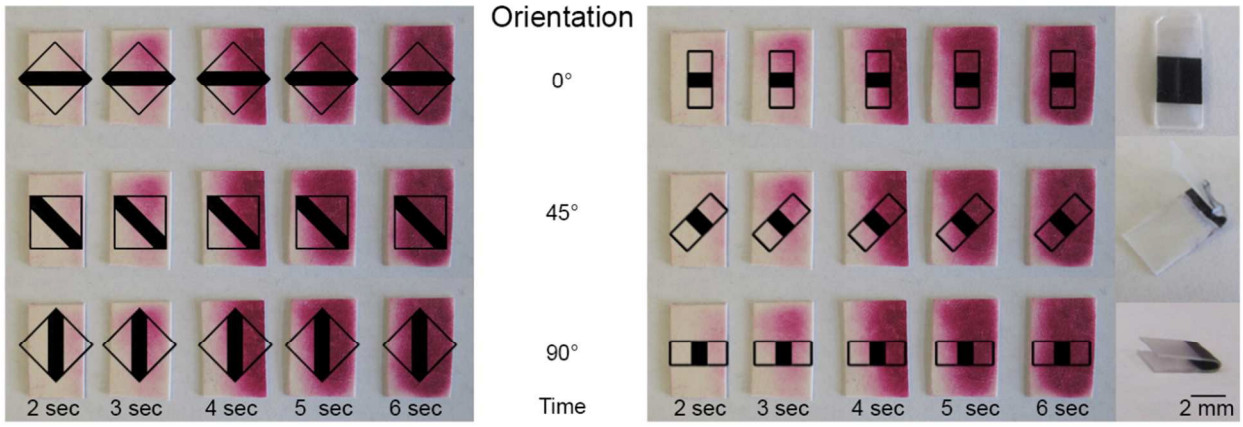

Figure 7. Microwave sensitive paper changes color when heated by microwaves to show the non-uniformity of microwaves. Depictions of the polymer samples are superimposed over the paper for the sake of visualization. The microwaves heat non-uniformly, which explains why the hinges at 90° orientation fold and 0 and 45° deform, as shown in the photographs located in the right-most column.

For the sake of visualization, **Figure 7** superimposes the geometry and orientation of the hinges (which were not present while heating the paper). It also displays the three types of folding behaviors observed as a result of orientation in otherwise identical samples. The 0° sample shows the beginnings of 'cratering'; portions of the polymer in the hinge region flow away from the hinge, but the sample does not fold due to the physical restraint offered by the portions of the hinge that remain below the T_g of the sheet. The 45° sample folds unevenly. The 90° samples fold very well (cf. **Figure 2**). There results highlight the effects of non-uniform heating on the folding process.

To gain a better understanding of the response of the samples to microwave induced heating we modeled the folding process using Abaqus finite element analysis software. The model is based primarily on a model developed for the self-folding of pre-strained polystyrene sheets that fold due to IR induced heating(73). Briefly, the model starts by pre-straining the polymer sheet at an elevated temperature prior to cooling the sheet to preserve the pre-strained state. From the pre-strained state, we impose representative thermal and mechanical boundary conditions. The temperature distribution measured experimentally across the surface of the samples serves

as a thermal boundary condition. The model predicts the resulting deformation based on the strain relaxation of the polymer in response to this thermal profile. Square and diagonal hinge geometries are modeled each with 6 mm wide hinges oriented at a 90° azimuthal angle. **Figure 8** shows representative results from these simulations.

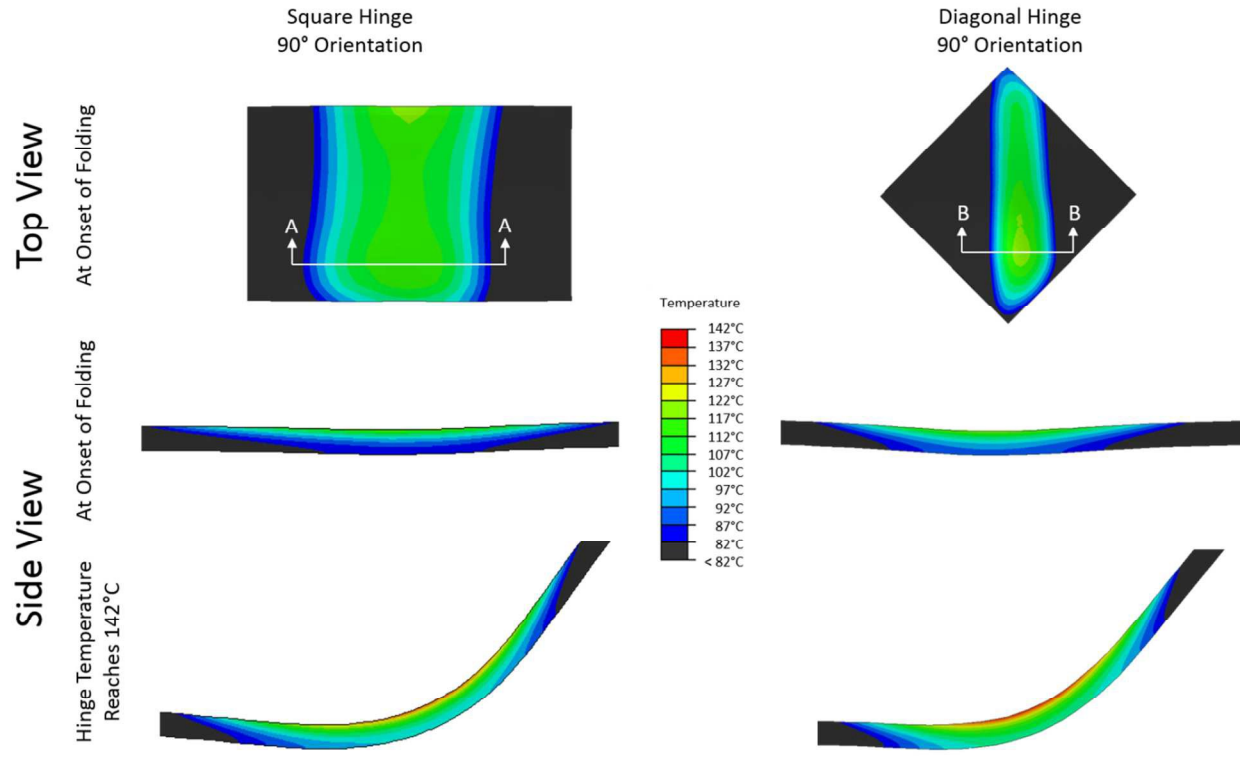

Figure 8. Results from Abaqus model that show the temperature profile on the surface (top view) and through the thickness of the samples (side view) oriented at 90°. The images truncate the regions outside the hinge region for better visualization of the thermal profile of the hinge. The side view images are expanded to the distance 'A' and 'B' (which are equal). The black portion of the image is the edge of the unheated polymer.

At the onset of folding (middle row in **Figure 8**) the maximum patterned surface temperature for both hinge geometries is ~117°C while the bottom surface is ~82°C, a difference of 35°C. Later in the folding process, when the patterned surface temperature reaches ~142°C (bottom row in **Figure 8**), the temperature on the bottom surface is ~102°C, a difference of 40°C. This temperature gradient is double the temperature gradient seen in IR induced folding samples(24). The folding happens within seconds because the microwaves efficiently deliver large amounts of heat locally to a patterned hinge. Although the bottom of the sample approaches T_g during folding, the onset of folding occurs when the bottom of the microwave sample is significantly below T_g. Folding of the sample prior to the bottom surface reaching T_g is

due to the large temperature gradient in the microwave samples, which is remarkably large considering the sheets are only ~300 μm thick.

Conclusions

This paper demonstrates self-folding of pre-strained polymer films using microwaves as a heating source. A pattern of graphene ink on the surface of pre-strained polymer films absorbs the microwaves and causes the polymer to shrink directly below the hinge, which induces the polymer sheet to fold. The dihedral angle is directly proportional to the hinge width printed on the polymer sheet and it is possible to self-fold all the way to 180°. The quality of the folding depends on the geometry and orientation of the sample due to uneven distribution of microwaves energy in the microwave reactor (commercial microwaves also have non-uniform heating). The best folding occurs when the hinge receives as uniform heating as possible across its length, which occurs at an azimuthal sample orientation of 90° within the reactor. A finite element model suggest that the absorption of microwave energy by the hinge results in a temperature difference of ~40 °C from top to bottom of the polymer samples. This large temperature difference explains why the samples are able to fold within seconds despite starting at room temperature.

Polymer sheets that fold in response to microwaves could have several applications, particularly since microwaves are common household items. Here, we utilize graphene inks, but it is possible to use other microwave absorbers including materials that might be optically transparent. This technique folds polymers quickly and accurately which lends itself to time sensitive applications. This technique could be used for triggering remote folding or for activating folding within enclosures or through materials transparent to microwaves.

Acknowledgements

The authors thank the National Science Foundation for supporting this work under the NSF EFRI program (Grant No. 1240438). We also thank Professor Chris Gorman for access to his CEM LabMate microwave, Progressive Graphics (http://www.progressivegraphics.net) for their screen printing expertise, and our EFRI Collaborators for their constructive feedback. Supporting Information is available online.

Experimental Section

Onto Shrinky-Dink™ sheets (prestrained polystyrene), we screen printed Vor-ink™ (graphene ink) as straight lines using a 180 mesh screen. The lines define the 'hinges' and have widths from 1 – 6 mm. Next, we laser cut two different sized samples from the inked sheets: 13 mm x 13 mm and 13 mm x 6 mm rectangles. We placed the samples onto a CEM Discover microwave oven and heated the samples at 250 W. We tested three different physical orientations (0°, 45°, and 90°) up to 60 seconds (although most trials ended much earlier). We used an IR camera to record the surface temperature profiles.

References

1. Taylor D, Dyer D, Lew V, Khine M. Shrink film patterning by craft cutter: complete plastic chips with high resolution/high-aspect ratio channel. Lab Chip. 2010 Aug 25;10(18):2472–5.

2. Lin S, Lee EK, Nguyen N, Khine M. Thermally-induced miniaturization for micro- and nanofabrication: progress and updates. Lab Chip. 2014 Jul 14;14(18):3475–88.

3. Grimes A, Breslauer DN, Long M, Pegan J, Lee LP, Khine M. Shrinky-Dink microfluidics: rapid generation of deep and rounded patterns. Lab Chip. 2008;8(1):170.

4. Hayes GJ, Liu Y, Genzer J, Lazzi G, Dickey MD. Self-Folding Origami Microstrip Antennas. IEEE Trans Antennas Propag. 2014;62(10):5416–9.

5. Fernandes R, Gracias DH. Self-folding polymeric containers for encapsulation and delivery of drugs. Adv Drug Deliv Rev. 2012;64(14):1579–89.

6. Felton S, Tolley M, Demaine E, Rus D, Wood R. A method for building self-folding machines. Science. 2014;345(6197):644–6.

7. Wood RJ, Avadhanula S, Sahai R, Steltz E, Fearing RS. Microrobot Design Using Fiber Reinforced Composites. J Mech Des. 2008;130(5):052304–052304.

8. Silverberg JL, Evans AA, McLeod L, Hayward RC, Hull T, Santangelo CD, et al. Using origami design principles to fold reprogrammable mechanical metamaterials. Science. 2014;345(6197):647–50.

9. Bothe M, Pretsch T. Bidirectional actuation of a thermoplastic polyurethane elastomer. J Mater Chem A. 2013;1(46):14491–7.

10. Ikeda T, Nakano M, Yu Y, Tsutsumi O, Kanazawa A. Anisotropic Bending and Unbending Behavior of Azobenzene Liquid-Crystalline Gels by Light Exposure. Adv Mater. 2003;15(3):201–5.

11. Leng J, Wu X, Liu Y. Infrared light-active shape memory polymer filled with nanocarbon particles. J Appl Polym Sci. 2009;114(4):2455–60.

12. Lee KM, Koerner H, Vaia RA, Bunning TJ, White TJ. Light-activated shape memory of glassy, azobenzene liquid crystalline polymer networks. Soft Matter. 2011;7(9):4318–24.

13. Beblo RV, Weiland LM. Light Activated Shape Memory Polymer Characterization. J Appl Mech-Trans Asme. 2009;76(1).

14. Zhang H, Xia H, Zhao Y. Light-Controlled Complex Deformation and Motion of Shape-Memory Polymers Using a Temperature Gradient. ACS Macro Lett. 2014;940–3.

15. Wang E, Desai MS, Lee S-W. Light-Controlled Graphene-Elastin Composite Hydrogel Actuators. Nano Lett. 2013;13(6):2826–30.

16. Li M-H, Keller P, Li B, Wang X, Brunet M. Light-Driven Side-On Nematic Elastomer Actuators. Adv Mater. 2003;15(78):569–72.

17. Lendlein A, Jiang H, Juenger O, Langer R. Light-induced shape-memory polymers. Nature. 2005;434(7035):879–82.

18. Habault D, Zhang H, Zhao Y. Light-triggered self-healing and shape-memory polymers. Chem Soc Rev. 2013;42(17):7244–56.

19. Sodhi JS, Rao IJ. Modeling the mechanics of light activated shape memory polymers. Int J Eng Sci. 2010;48(11):1576–89.

20. Ryu J, D'Amato M, Cui X, Long KN, Qi HJ, Dunn ML. Photo-origami—Bending and folding polymers with light. Appl Phys Lett. 2012;100(16):161908/1–5.

21. Jiang W, Niu D, Liu H, Wang C, Zhao T, Yin L, et al. Photoresponsive Soft-Robotic Platform: Biomimetic Fabrication and Remote Actuation. Adv Funct Mater. 2014;

22. Jiang HY, Kelch S, Lendlein A. Polymers Move in Response to Light. Adv Mater. 2006;18(11):1471–5.

23. Zhang H, Zhao Y. Polymers with Dual Light-Triggered Functions of Shape Memory and Healing Using Gold Nanoparticles. ACS Appl Mater Interfaces. 2013;

24. Liu Y, Boyles JK, Genzer J, Dickey MD. Self-folding of polymer sheets using local light absorption. Soft Matter. 2012;8(6):1764–9.

25. Gracias DH. Stimuli responsive self-folding using thin polymer films. Curr Opin Chem Eng. 2013;2(1):112–9.

26. Chatani S, Kloxin CJ, Bowman CN. The power of light in polymer science: photochemical processes to manipulate polymer formation, structure, and properties. Polym Chem. 2014;5(7):2187–201.

27. Meng H, Mohamadian H, Stubblefield M, Jerro D, Ibekwe S, Pang S-S, et al. Various shape memory effects of stimuli-responsive shape memory polymers. Smart Mater Struct. 2013;22(9).

28. Lucas TM, James KT, Beharic J, Moiseeva EV, Keynton RS, O'Toole MG, et al. Wavelength specific excitation of gold nanoparticle thin-films. Appl Phys Lett. 2014;104(1):011909.

29. Na J-H, Evans AA, Bae J, Chiappelli MC, Santangelo CD, Lang RJ, et al. Programming Reversibly Self-Folding Origami with Micropatterned Photo-Crosslinkable Polymer Trilayers. Adv Mater. 2015;27(1):79–85.

30. Nguyen TD, Jerry Qi H, Castro F, Long KN. A thermoviscoelastic model for amorphous shape memory polymers: incorporating structural and stress relaxation. J Mech Phys Solids. 2008;56(9):2792–814.

31. Stroganov V, Zakharchenko S, Sperling E, Meyer AK, Schmidt OG, Ionov L. Biodegradable Self-Folding Polymer Films with Controlled Thermo-Triggered Folding. Adv Funct Mater. 2014;24(27):4357–63.

32. Qi HJ, Nguyen TD, Castro F, Yakacki CM, Shandas R. Finite deformation thermo-mechanical behavior of thermally induced shape memory polymers. J Mech Phys Solids. 2008;56(5):1730–51.

33. Diani J, Liu Y, Gall K. Finite strain 3D thermoviscoelastic constitutive model for shape memory polymers. Polym Eng Sci. 2006;46(4):486–92.

34. Diani J, Gilormini P, Frédy C, Rousseau I. Predicting thermal shape memory of crosslinked polymer networks from linear viscoelasticity. Int J Solids Struct. 2012;49(5):793–9.

35. Xu B, Fu YQ, Ahmad M, Luo JK, Huang W, Kraft A, et al. Thermo-mechanical properties of polystyrene-based shape memory nanocomposites. J Mater Chem. 2010;20(17):3442.

36. Tamagawa H. Thermo-responsive two-way shape changeable polymeric laminate. Mater Lett. 2010 Mar;64(6):749–51.

37. Hawkes E, An B, Benbernou NM, Tanaka H, Kim S, Demaine ED, et al. Programmable matter by folding. Proc Natl Acad Sci. 2010;

38. White TJ, Tabiryan NV, Serak SV, Hrozhyk UA, Tondiglia VP, Koerner H, et al. A high frequency photodriven polymer oscillator. Soft Matter. 2008;4(9):1796–8.

39. Liu Y, Miskiewicz M, Escuti MJ, Genzer J, Dickey MD. Three-dimensional folding of pre-strained polymer sheets via absorption of laser light. J Appl Phys. 2014;115(20).

40. Small W, Wilson TS, Benett WJ, Loge JM, Maitland DJ. Laser-activated shape memory polymer intravascular thrombectomy device. Opt Express. 2005;13(20):8204–13.

41. Piqué A, Mathews SA, Charipar NA, Birnbaum AJ. Laser origami: a new technique for assembling 3D microstructures. In: Bachmann FG, Pfleging W, Washio K, Amako J, Hoving W, Lu Y, editors. 2012.

42. Laflin KE, Morris CJ, Muqeem T, Gracias DH. Laser triggered sequential folding of microstructures. Appl Phys Lett. 2012;101(13):131901/1–4.

43. Alberto Piqué SAM. Laser Origami: a New Technique for Assembling 3D Microstructures. SPIE Proc Vol 8244. 2012;

44. de Haan LT, Gimenez-Pinto V, Konya A, Nguyen T-S, Verjans JMN, Sánchez-Somolinos C, et al. Accordion-like Actuators of Multiple 3D Patterned Liquid Crystal Polymer Films. Adv Funct Mater. 2014;24(9):1251–8.

45. Kim J, Hanna JA, Byun M, Santangelo CD, Hayward RC. Designing Responsive Buckled Surfaces by Halftone Gel Lithography. Science. 2012;335(6073):1201–5.

46. Guan JJ, He HY, Hansford DJ, Lee LJ. Self-folding of three-dimensional hydrogel microstructures. J Phys Chem B. 2005;109(49):23134–7.

47. Stoychev G, Zakharchenko S, Turcaud S, Dunlop JWC, Ionov L. Shape-Programmed Folding of Stimuli-Responsive Polymer Bilayers. ACS Nano. 2012;6(5):3925–34.

48. Chen D, Yoon J, Chandra D, Crosby AJ, Hayward RC. Stimuli-responsive buckling mechanics of polymer films. J Polym Sci Part B Polym Phys. 2014;52(22):1441–61.

49. Velankar SS, Lai V, Vaia RA. Swelling-Induced Delamination Causes Folding of Surface-Tethered Polymer Gels. ACS Appl Mater Interfaces. 2012;4(1):24–9.

50. Kim J, Hanna JA, Hayward RC, Santangelo CD. Thermally responsive rolling of thin gel strips with discrete variations in swelling. Soft Matter. 2012;8(8):2375–81.

51. Hsu Y-J, Jia Z, Kymissis I. A Locally Amplified Strain Sensor Based on a Piezoelectric Polymer and Organic Field-Effect Transistors. IEEE Trans Electron Devices. 2011;58(3):910–7.

52. Tanaka T, Nishio I, Sun S-T, Ueno-Nishio S. Collapse of Gels in an Electric Field. Science. 1982;218(4571):467–9.

53. Stellman P, Buchner T, Arora WJ, Barbastathis G. Dynamics of nanostructured Origami. J Microelectromechanical Syst. 2007;16(4):932–49.

54. Biggs J, Danielmeier K, Hitzbleck J, Krause J, Kridl T, Nowak S, et al. Electroactive Polymers: Developments of and Perspectives for Dielectric Elastomers. Angew Chem Int Ed. 2013;52(36):9409–21.

55. van den Ende D, Kamminga J-D, Boersma A, Andritsch T, Steeneken PG. Voltage-Controlled Surface Wrinkling of Elastomeric Coatings. Adv Mater. 2013;25(25):3438–42.

56. McGough K, Ahmed S, Frecker M, Ounaies Z. Finite element analysis and validation of dielectric elastomer actuators used for active origami - Abstract - Smart Materials and Structures - IOPscience. 2014.

57. Felton SM, Tolley MT, Shin B, Onal CD, Demaine ED, Rus D, et al. Self-folding with shape memory composites. Soft Matter. 2013;9(32):7688–94.

58. In HJ, Lee H, Nichol AJ, Kim SG, Barbastathis G. Carbon nanotube-based magnetic actuation of origami membranes. J Vac Sci Technol B. 2008;26(6):2509–12.

59. Yi YW, Liu C. Magnetic actuation of hinged microstructures. J Microelectromechanical Syst. 1999;8(1):10–7.

60. Judy JW, Muller RS. Magnetically actuated, addressable microstructures. J Microelectromechanical Syst. 1997;6(3):249–56.

61. Nguyen VQ, Ahmed AS, Ramanujan RV. Morphing Soft Magnetic Composites. Adv Mater. 2012;24(30):4041–54.

62. Martinez RV, Fish CR, Chen X, Whitesides GM. Elastomeric Origami: Programmable Paper-Elastomer Composites as Pneumatic Actuators. Adv Funct Mater.

63. Kwok SW, Morin SA, Mosadegh B, So J-H, Shepherd RF, Martinez RV, et al. Magnetic Assembly of Soft Robots with Hard Components. Adv Funct Mater. 2013;

64. Zheng L, Yoshida S, Morimoto Y, Onoe H, Takeuchi S. Pneumatic balloon actuator with tunable bending points. In: 2015 28th IEEE International Conference on Micro Electro Mechanical Systems (MEMS). 2015.

65. Liu Y, Genzer J, Dickey MD. 2D or not 2D: Shape Programming of Polymer Sheets. Prog Polym Sci. In Press 2015.

66. Krishna KVG. A method of determining the dipole moment and relaxation time from microwave measurements. Trans Faraday Soc. 1957;53(0):767–70.

67. Gabriel C, Gabriel S, Grant EH, Grant EH, Halstead BSJ, Mingos DMP. Dielectric parameters relevant to microwave dielectric heating. Chem Soc Rev. 1998;27(3):213–24.

68. Das CK, Bhattacharya P, Kalra SS. Graphene and MWCNT: Potential Candidate for Microwave Absorbing Materials. J Mater Sci Res. 2012;1(2).

69. Nüchter M, Ondruschka B, Bonrath W, Gum A. Microwave assisted synthesis – a critical technology overview. Green Chem. 2004;6(3):128–41.

70. Dakin TW, Works CN. Microwave Dielectric Measurements. J Appl Phys. 1947;18(9):789–96.

71. Hu H, Zhao Z, Zhou Q, Gogotsi Y, Qiu J. The role of microwave absorption on formation of graphene from graphite oxide. Carbon. 2012;50(9):3267–73.

72. Gokirmak A, Wu D-H, Bridgewater JSA, Anlage SM. A Scanned Perturbation Technique For Imaging Electromagnetic Standing Wave Patterns of Microwave Cavities. Rev Sci Instrum. 1998;69(9):3410.

73. Mailen RW, Liu Y, Dickey MD, Zikry M, Genzer J. Modelling of shape memory polymer sheets that self-fold in response to localized heating. Soft Matter. 2015;